Albumin Oxidation to Diverse Radicals by the Peroxidase Activity of Cu,Zn−Superoxide Dismutase in the Presence of Bicarbonate or Nitrite: Diffusible Radicals Produce Cysteinyl and Solvent-Exposed and -Unexposed Tyrosyl Radicals†

Marcelo G. Bonini, Denise C. Fernandes, and Ohara Augusto*

Departamento de Bioquímica, Instituto de Química, Universidade de São Paulo, CP 26077, CEP 05513-970, São Paulo, SP, Brazil

Received September 5, 2003; Revised Manuscript Received October 30, 2003

ABSTRACT: The peroxidase activity of Cu,Zn-superoxide dismutase (Cu,Zn-SOD) has been extensively studied in recent years due to its potential relationship to familial amyothrophic lateral sclerosis. The mechanism by which Cu,Zn-SOD/hydrogen peroxide/bicarbonate is able to oxidize substrates has been proposed to be dependent on an oxidant whose nature, diffusible carbonate radical anion or enzyme-bound peroxycarbonate, remains debatable. One possibility to distinguish these species is to examine whether protein targets are oxidized to protein radicals. Here, we used EPR methodologies to study bovine serum albumin (BSA) oxidation by Cu,Zn-SOD/hydrogen peroxide in the absence and presence of bicarbonate or nitrite. The results showed that BSA oxidation in the presence of bicarbonate or nitrite at pH 7.4 produced mainly solvent-exposed and -unexposed BSA-tyrosyl radicals, respectively. Production of the latter was shown to be preceded by BSA-cysteinyl radical formation. The results also showed that hydrogen peroxide/bicarbonate extensively oxidized BSA-cysteine to the corresponding sulfenic acid even in the absence of Cu,Zn-SOD. Thus, our studies support the idea that peroxycarbonate acts as a two-electron oxidant and may be an important biological mediator. Overall, the results prove the diffusible and radical nature of the oxidants produced during the peroxidase activity of Cu,Zn-SOD in the presence of bicarbonate or nitrite.

Copper−zinc superoxide dismutase is an abundant eukaryotic cytosolic enzyme that efficiently catalyzes the disproportionation of $O_2^{\bullet-}$ into O_2 and H_2O_2 through redox cycling of its catalytic copper ion (*1*). In addition to its normal reaction with $O_2^{\bullet-}$, Cu,Zn-SOD can react with H_2O_2 to generate a powerful oxidant that can attack the enzyme itself and can oxidize exogenous substrates (*2*−*6*). This peroxidase activity of the enzyme has been extensively studied in recent years due to its potential relationship with mutated varieties of SOD[1] that cause some cases of the fatal motor neuron disease, familial amyothrophic lateral sclerosis (*7*−*10*).

The peroxidative mechanism of Cu,Zn-SOD remains debatable, but the formation of a copper-bound one-electron oxidant (Cu(II)$^{\bullet}$OH, Cu(I)O, or Cu(III)) accounts for most of the experimental data (eqs 1−6) (*3*, *4*, *6*, *11*−*15*). For instance, enzyme inactivation has been proposed to result from the oxidation of a histidine residue adjacent to the copper-bound one-electron oxidant (eq 4). The requirement of HCO_3^- for the oxidation of substrates such as NADPH and DMPO that are unlikely to have access to the Cu,Zn-SOD active site has been attributed to HCO_3^- oxidation to $CO_3^{\bullet-}$ (eq 5) that diffuses away from the enzyme. Accordingly, Kalyanaraman and co-workers presented strong evidences that Cu,Zn-SOD/hydrogen peroxide is able to oxidize HCO_3^- (eq 5) (*12*, *13*, *15*) and NO_2^- (eq 6) (*11*) to diffusible $CO_3^{\bullet-}$ and $^{\bullet}NO_2$, respectively.

$$\text{SOD-Cu(II)} + H_2O_2 \rightleftarrows \text{SOD-Cu(I)} + O_2^{\bullet-} + 2H^+ \quad (1)$$

$$\text{SOD-Cu(I)} + H_2O_2 \rightleftarrows \text{SOD-Cu(II)}^{\bullet}\text{OH} + {}^{-}\text{OH} \quad (2)$$

$$\text{SOD-Cu(II)} + O_2^{\bullet-} \rightarrow \text{SOD-Cu(I)} + O_2 \quad (3)$$

$$\text{SOD-Cu(II)}^{\bullet}\text{OH} + \text{SOD-His} \rightarrow \text{SOD-Cu(II)} + \text{SOD-}^{\bullet}\text{His} \quad (4)$$

$$\text{SOD-Cu(II)}^{\bullet}\text{OH} + HCO_3^- \rightarrow \text{SOD-Cu(II)} + H_2O + CO_3^{\bullet-} \quad (5)$$

$$\text{SOD-Cu(II)}^{\bullet}\text{OH} + NO_2^- \rightarrow \text{SOD-Cu(II)} + H_2O + {}^{\bullet}NO_2 \quad (6)$$

More recently, however, Elam and co-workers have proposed that the oxidant produced from Cu,Zn-SOD/H_2O_2 in the presence of HCO_3^- is firmly bound to the enzyme and

† This work was supported by grants from the Fundação de Amparo à Pesquisa do Estado de São Paulo (FAPESP), Conselho Nacional de Desenvolvimento Científico e Tecnológico (CNPq), and Financiadora de Estudos e Projetos (FINEP).

* To whom correspondence should be addressed. Phone: 55-11-3091-3873. Fax: 55-11-30912186 and 55-11-3815-5579. E-mail: oaugusto@iq.usp.br.

[1] Abbreviations: BSA, bovine serum albumin; BSA-cysSH, bovine serum albumin free thiol group; BSA-cysSOH, the sulfenic acid of bovine serum albumin; DBNBS, 3,5-dibromo-4-nitrosobenzenesulfonic acid; DTNB, 5,5′-dithio-bis(2-nitrobenzoic acid); DMPO, 5,5-dimethyl-pirroline-1-oxide; NBD-Cl, 7-chloro-4-nitrobenzeno-2-oxa-1,3-diazol; SOD, superoxide dismutase.

10.1021/bi035606p CCC: $27.50
Published on Web 12/17/2003

formed from an enzyme-associated peroxycarbonate (HCO_4^-) intermediate (*16*).

Peroxycarbonate is a known oxidant that is likely to act by two-electron mechanisms (*17*, *18*) except in the presence of redox active transition metal ions (*19*, *20*). The copper ion in the Cu,Zn-SOD active site can certainly intermediate the production of $CO_3^{\bullet-}$ from HCO_4^- (*16*). If the latter leaves the active site, however, it is likely to oxidize external targets by two-electron mechanisms (*17*, *18*). As mentioned before, there is evidence that the oxidant produced from Cu,Zn-SOD/H_2O_2/HCO_3^- or Cu,Zn-SOD/H_2O_2/NO_2^- oxidizes external targets by one-electron mechanisms (*11*, *13*−*15*, *16*). This evidence, however, is limited to these few cases because most of the other studies have monitored either enzyme inactivation or overall substrate oxidation and not substrate oxidation to radicals (*2*−*4*, *14*, *16*). Certainly, the oxidants produced from the peroxidase activity of Cu,Zn-SOD in the presence of HCO_3^- or NO_2^- deserve further studies.

Particularly relevant is the examination of whether these oxidants can oxidize target proteins to protein-derived radicals. On one hand, oxidized proteins have been detected in transgenic mice expressing a familial amyothrophic lateral sclerosis-associated mutant human Cu,Zn-SOD (*21*, *22*), suggesting that protein radicals and their resulting products may contribute to the development of the disease. On the other hand, a target protein is certainly excluded from the Cu,Zn-SOD active site, and its oxidation to protein radicals will require diffusible oxidants that are, themselves, radicals. Here, we used direct EPR and EPR spin trapping to demonstrate that BSA is oxidized to protein radicals by Cu,Zn-SOD/H_2O_2/HCO_3^- and Cu,Zn-SOD/H_2O_2/NO_2^-. The main produced BSA radicals were characterized and shown to be consistent with BSA attack by either $CO_3^{\bullet-}$ or $^{\bullet}NO_2$, respectively. Incidentally, the studies also presented evidences for the production of HCO_4^- from H_2O_2 and HCO_3^- and for its action as a two-electron oxidant.

EXPERIMENTAL PROCEDURES

Chemicals. All reagents were purchased from Sigma, Aldrich, Merck, or Fisher and were analytical grade or better. Cu,Zn-SOD from bovine erythrocytes was from Roche Applied Science. DMPO was purified by distillation. DBNBS was synthesized from 3,5-dibromosulfanilic acid sodium salt as previously described (*23*). All buffers were pretreated with Chellex-100 to remove metal ion contamination. All solutions were prepared with distilled water purified with a Millipore Milli-Q system.

Solutions and Incubations. BSA (fraction V) from Merck was treated overnight with 10× molar excess of 2-mercaptoethanol at 4 °C to reduce thiol residues. Excess reductant was removed by dialysis against 0.01 and 0.25 M phosphate buffers, pH 7.4. BSA solutions thus prepared were 1.5−2.0 mM and typically 0.7−0.9 BSA-cysSH/BSA. In the case of some experiments, the BSA-cysSH was blocked by previous treatment with *N*-ethylmaleimide (*24*). Hydrogen peroxide concentration was determined spectrophotometrically at 240 nm using an extinction coefficient of 43.6 M^{-1} cm^{-1} (*25*). Concentrations of CO_2 were calculated from the added HCO_3^- concentrations by using $pK_a = 6.4$ (*26*). All incubations were performed in 250 mM phosphate buffer, pH 7.4 at 25 ± 2 °C.

Assay of Cu,Zn-SOD Activity. Aliquots of the reaction mixtures were taken at various incubation times, and the reaction was stopped by dilution with a solution containing catalase to a final concentration of 20 units/mL. Cu,Zn-SOD activity was measured by cytochrome *c* reduction as previously described (*15*).

Thiol Oxidation. Aliquots of the reaction mixtures were taken at various incubation times, and the reaction was stopped by dilution with phosphate buffer, pH 8.0 containing catalase (20 units/mL) and DTBN (1 mM). After a further 20 min incubation, the thiol concentration was determined by spectrophotometric quantitation of 5-thio-2-nitrobenzoate at 412 nm ($\epsilon = 13.6 \times 10^3$ M^{-1} cm^{-1}) (*26*).

Trapping of Sulfenic Acid with NBD-Cl. Aliquots of the reaction mixtures were taken at various incubation times, and the reaction was stopped by dilution with a solution containing catalase to a final concentration of 20 units/mL. NDB-Cl (0.1 mM) (2× molar excess over BSA) was added to the samples, and after 30 min incubation, they were filtered through centricon filters (10 kDa cutoff) and washed two times with phosphate buffer. The UV−vis spectra of the resuspended samples were recorded with an upgraded Aminco SL 2000 spectrophotometer.

EPR Experiments. The EPR experiments were performed at room temperature on a Bruker EMX spectrometer operating at 9.65 GHz and 100 kHz field modulation. The reaction mixtures were transferred to a 200 μL flat cell immediately after hydrogen peroxide addition, and the spectra were recorded at various incubation times. The protein radical concentrations were estimated by double integration of EPR spectra using known concentrations of 4-hydroxy-2,2,6,6-tetramethyl-1-piperidinyloxy radical solutions in glycerol as standard.

RESULTS

Direct EPR Studies. Incubations of BSA (100 mg/mL) with Cu,Zn-SOD (2.5 mg/mL) in the presence of H_2O_2 (2.5 mM) and HCO_3^- (25 mM) led to the detection of a broad and relatively intense EPR spectrum that is characteristic of a protein-bound radical (Figure 1). Signal detection was dependent on the presence of all incubation components, and signal intensity increased with the concentrations of HCO_3^- (10−50 mM) (Figure 1), H_2O_2 (0.5−5 mM), and Cu,Zn-SOD (1.0−7.5 mg/mL) but was marginally affected by BSA concentrations higher than 25 mg/mL (data not shown). The EPR parameters of the detected radical ($g = 2.004$; total line width of 49 G) (Figure 1) were consistent with those of protein-Tyr$^{\bullet}$ radicals (*27*−*29*). Since the radical was not detectable in the absence of BSA, it could then be characterized as a BSA-Tyr$^{\bullet}$ radical. The fact that this radical is detectable at room temperature and under air also argues for a BSA-Tyr$^{\bullet}$ because all the other protein residues that are prone to one-electron oxidation produce radicals that react extremely quickly with oxygen and are not detectable by static direct EPR at room temperature (*29*). Accordingly, the spectrum shown in Figure 1 is very similar to the BSA-Tyr$^{\bullet}$ radical obtained in incubations of BSA with horseradish peroxidase/H_2O_2 (*28*). The EPR signal was typically detected 1 min after H_2O_2 addition and was observed for more than 60 min without significant alteration of its intensity (Figure 2, full bars). Two factors are likely to be contributing to this

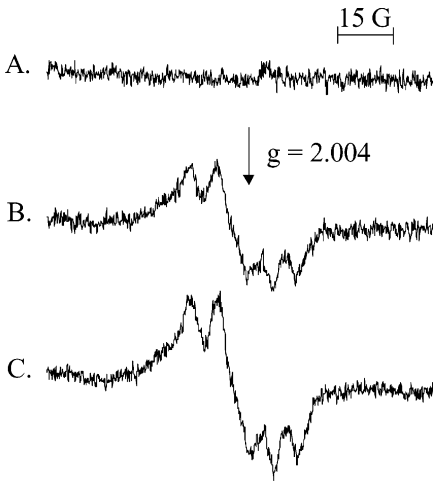

FIGURE 1: Direct EPR spectrum of the BSA-derived radical produced in incubations of BSA (100 mg/mL), Cu,Zn-SOD (2.5 mg/mL), and H_2O_2 (2.5 mM) in phosphate buffer (250 mM), pH 7.4. (A) In the absence of HCO_3^-; (B) in the presence of 25 mM HCO_3^-; and (C) in the presence of 50 mM HCO_3^-. The spectra were recorded 1 min after H_2O_2 addition. Instrumental conditions: microwave power, 20 mW; modulation amplitude, 2.5 G; time constant, 327.68 ms; scan rate, 0.3 G/s; and gain, 4.48×10^5.

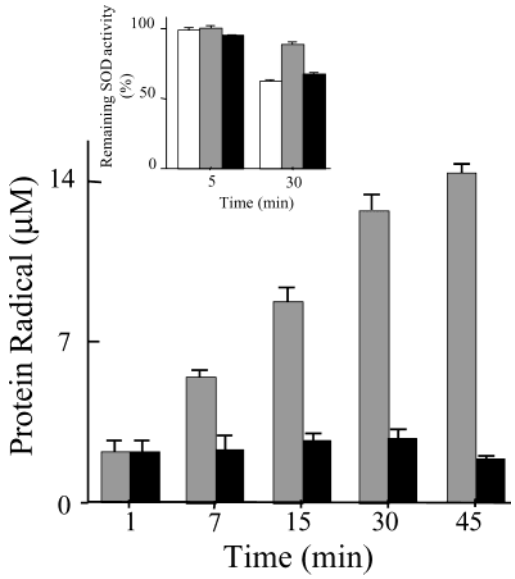

FIGURE 2: Variation of BSA-derived radical concentration with incubation time. Radicals were detected by direct EPR analysis of incubations of BSA (100 mg/mL), Cu,Zn-SOD (2.5 mg/mL), and H_2O_2 (2.5 mM) in phosphate buffer (250 mM), pH 7.4, containing HCO_3^- (50 mM) (full bars) or NO_2^- (50 mM) (gray bars). The inset shows the variation of Cu,Zn-SOD activity with incubation time of mixtures containing the same concentrations as above of Cu,Zn-SOD/H_2O_2 (open bars); Cu,Zn-SOD/H_2O_2/HCO_3^- (full bars); and Cu,Zn-SOD/H_2O_2/NO_2^- (gray bars). Radical concentrations and Cu,Zn-SOD activity were estimated as described in the Experimental Procedures. The shown values are mean ± standard deviations of the values obtained in three independent experiments.

behavior. One is the hydrogen peroxide-mediated inactivation of Cu,Zn-SOD (*2*, *3*, *6*, *14*). Indeed, after 30 min incubation, the enzyme lost 40% of its activity toward $O_2^{\bullet -}$ dismutation in the absence of HCO_3^-, and the anion protected the enzyme to a marginal extent (Figure 2, inset), in agreement with recent studies by Liochev and Fridovich (*14*). The second factor is probably the half-life of the detected BSA-Tyr$^\bullet$ radical. Although it may appear long-lived because it is

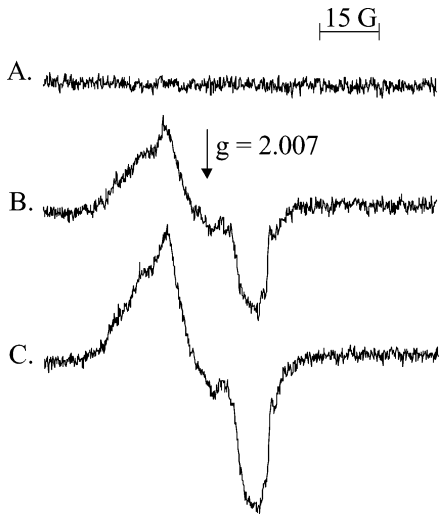

FIGURE 3: Direct EPR spectrum of the BSA-derived radical produced in incubations of BSA (100 mg/mL), Cu,Zn-SOD (2.5 mg/mL), and H_2O_2 (2.5 mM) in phosphate buffer (250 mM), pH 7.4. (A) In the absence of NO_2^-; (B) in the presence of 25 mM NO_2^-; and (C) in the presence of 50 mM NO_2^-. The spectra shown were recorded 1 min after H_2O_2 addition. Instrumental conditions: microwave power, 20 mW; modulation amplitude, 2.5 G; time constant, 327.68 ms; scan rate, 0.3 G/s; and gain, 4.48×10^5.

detectable at room temperature and under air, this appears to result from a similar rate of radical production and decay up to 30 min incubation (Figure 2, full bars). Accordingly, instantaneous radical concentrations decreased at longer incubations when the rate of radical production should decrease due to the pronounced enzyme inactivation (Figure 2).

The replacement of HCO_3^- by NO_2^- in incubations of Cu,Zn-SOD/H_2O_2/BSA led to the detection of a completely different EPR spectrum (Figure 3). Also in this case, signal detection was dependent on the presence of all incubation components, and its intensity varied with their concentrations. The EPR signal was broad and characteristic of a protein-bound radical, certainly a BSA-derived radical. The yields of this radical kept increasing up to 30 min incubation in sharp contrast with the behavior of the BSA-Tyr$^\bullet$ radical detected in the presence of HCO_3^- (Figure 2). This difference can be partially attributed to the protection afforded by NO_2^- on Cu,Zn-SOD inactivation by H_2O_2 (Figure 2, inset). In addition, the BSA-derived radical produced in the presence of NO_2^- is more stable than the one detected in the presence of HCO_3^- because it attained higher instantaneous concentrations at all incubation times except at the first minute (Figure 2). The EPR parameters of the BSA-bound radical detected in the presence of NO_2^- ($g = 2.007$; total line width of 54 G) (Figure 3) were also consistent with those of previously characterized protein-Tyr$^\bullet$ radicals (*27*).

BSA contains one free thiol group, cysteine34, that is easily oxidized by several agents to the corresponding cysteinyl radical (*24*, *26*, *30*, *31*). In some instances, the BSA-CysS$^\bullet$ radical has been shown to participate in intramolecular electron transfer producing other BSA-derived radicals while being reduced back to the thiol (*30*). On this basis, it was important to verify the effects of blocking BSA-CysSH on the BSA-derived radical production. As shown in Figure 4, the blockage of BSA-CysSH with *N*-ethylmaleimide com-

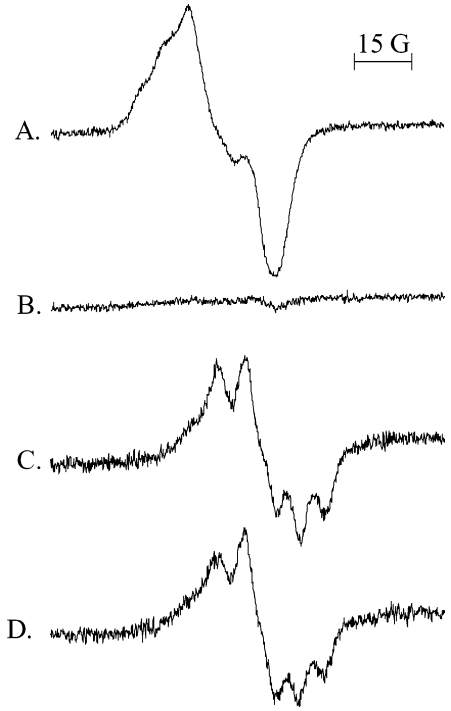

FIGURE 4: Direct EPR spectra of BSA-derived radicals produced in incubations containing native BSA-cysSH or BSA-cysS-NEM. The spectra were obtained from incubations of BSA (100 mg/mL), Cu,Zn-SOD (2.5 mg/mL), and H_2O_2 (2.5 mM) in phosphate buffer (250 mM), pH 7.4, in the presence of NO_2^- (50 mM) (A and B) or HCO_3^- (50 mM) (C and D). The spectra shown in panels A and C were obtained with native BSA-cysSH, whereas those shown in panels B and D were obtained with BSA-cys-NEM. The spectra were recorded 15 min after H_2O_2 addition. Instrumental conditions: microwave power, 20 mW; modulation amplitude, 2.5 G; time constant, 327.68 ms; scan rate, 0.3 G/s; and gain, 4.48×10^5.

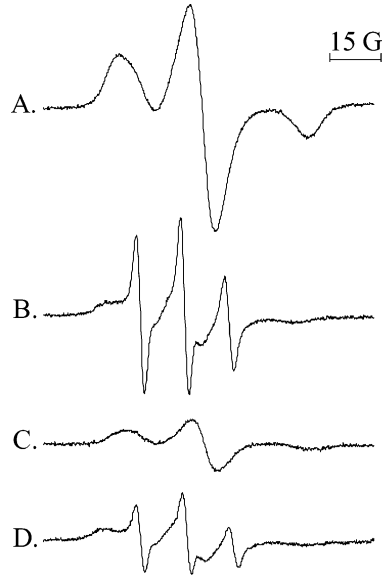

FIGURE 5: EPR spectra of DBNBS/$^{\bullet}$BSA and digested DBNBS/$^{\bullet}$BSA radical adducts. The spectra were obtained from incubations of BSA (100 mg/mL), Cu,Zn-SOD (2.5 mg/mL), H_2O_2 (2.5 mM), and DBNBS (20 mM) in phosphate buffer (250 mM), pH 7.4, containing HCO_3^- (50 mM) (A and B) or NO_2^- (50 mM) (C and D). DBNBS was added 15 min after H_2O_2 addition, and the spectra were scanned 1 min later. Spectra shown in panels B and D were obtained after digestion with proteinase K of the incubations shown in panels A and B, respectively. Instrumental conditions: microwave power, 20 mW; modulation amplitude, 2.5 G for spectra in A and C and 1.0 G for spectra in B and D; time constant 327.68 ms; scan rate, 0.6 G/s; and gain, 4.48×10^4.

pletely abolished the detection of the BSA-Tyr$^{\bullet}$ radical produced from native BSA incubated with Cu,Zn-SOD/H_2O_2/NO_2^- (Figure 4A,B). In contrast, native or blocked BSA produced the same BSA-Tyr$^{\bullet}$ radical when treated with Cu,Zn-SOD/H_2O_2/HCO_3^- (Figure 4C,D). These results indicate that production of BSA-CysS$^{\bullet}$ precedes the formation of the BSA-Tyr$^{\bullet}$ radical detected in the presence of NO_2^- but not of that detected in the presence of HCO_3^-.

The above direct EPR studies demonstrate that tyrosine residues located at different sites within the BSA structure are oxidized by Cu,Zn-SOD/H_2O_2/HCO_3^- or Cu,Zn-SOD/H_2O_2/NO_2^-(Figures 1−3). They also indicate that oxidation of cysteine34 to the BSA-CysS$^{\bullet}$ radical is likely to precede the production of the BSA-Tyr$^{\bullet}$ radical detected in NO_2^- presence (Figure 4). To obtain further information about the oxidized residues and their resulting radicals, spin trap experiments were performed.

Spin Trapping Experiments. First, a spin trap adequate for trapping protein-Tyr$^{\bullet}$ radicals, that is, DBNBS, was employed. DBNBS (20 mM) was added after 15 min of incubation when the radical formation appears to be steady by direct EPR (Figure 2) (*29*, *32*). Upon DBNBS addition, the radicals detected by direct EPR were replaced by broad triplets that are characteristic of DBNBS-protein radical adduct spectra (Figure 5). These adducts were digested with proteinase K and examined again by EPR. The resulting mobile triplet spectra (Figure 5B,D) presented a nitrogen hyperfine splitting constant (a_N) value of 13.6 G, which is consistent with that of both DBNBS/$^{\bullet}$Tyr and DBNBS/$^{\bullet}$Trp radical adducts (*33*). Thus, the a_N value alone could not discriminate between BSA-derived tyrosyl or tryptophanyl radicals. The fact that the same radicals were detectable by direct EPR (Figures 1 and 3) and trapped by DBNBS (Figure 5) (*29*, *32*), however, further supports the idea that the main radicals produced from BSA treated with Cu,Zn-SOD/H_2O_2 in the presence of HCO_3^- or NO_2^- are BSA-Tyr$^{\bullet}$ radicals. There was a striking difference in the intensities of the spectra of the DBNBS adducts produced in incubations containing HCO_3^- (Figure 4A) or NO_2^- (Figure 4C). The latter produced a considerable lower yield of DBNS/$^{\bullet}$Tyr-BSA radical adduct, in sharp contrast with the results obtained by direct EPR (Figures 1−3). This comparison indicates that the BSA-Tyr$^{\bullet}$ radical produced in incubations containing NO_2^- is less accessible to the spin trap and therefore less solvent-exposed than the one produced in the presence of HCO_3^-.

Spin trapping experiments were also performed with DMPO, which is an adequate trap to most radicals, including oxygen and sulfur centered radicals (*24*, *26*, *30*, *34*, *35*). DMPO, however, is usually less efficient than DBNBS in trapping protein-Tyr$^{\bullet}$ radicals (*34*, *36*). The detection of DMPO radical adducts in incubations of Cu,Zn-SOD/H_2O_2 and HCO_3^- or NO_2^- was more clear when the trap was added at zero time incubation; this was the procedure employed here. In HCO_3^- containing incubations, the EPR spectrum was again consistent with that of a DMPO/$^{\bullet}$Tyr-BSA radical adduct (a^{β}_H = 8.6 G) (Figure 6A) (*35*, *36*). In NO_2^- containing incubations, the spectrum obtained in the presence of DMPO (Figure 6B) was always dominated by the relatively stable BSA-Tyr$^{\bullet}$ radical detected in its absence

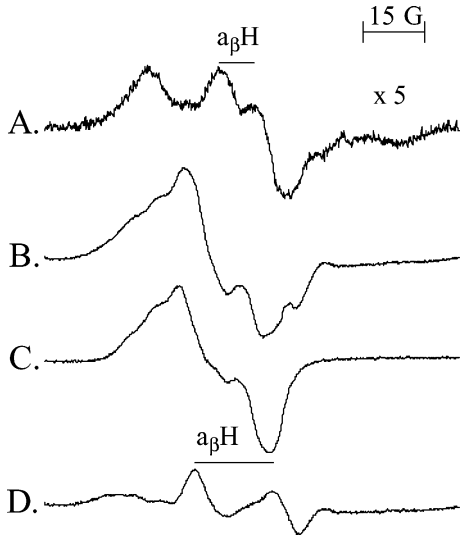

FIGURE 6: EPR spectra of DMPO•/BSA radical adducts. The spectra were obtained from incubations of BSA (100 mg/mL), Cu,Zn-SOD (2.5 mg/mL), H_2O_2 (2.5 mM), and DMPO (50 mM) in phosphate buffer (250 mM), pH 7.4, containing HCO_3^- (50 mM) (A) or NO_2^- (50 mM) (B and C). Spectrum D is the computer subtraction of B − C. The spectra were recorded 15 min after H_2O_2 addition. Instrumental conditions: microwave power, 20 mW; time constant, 327 ms; scan rate, 0.3 G/s; modulation amplitude, 2.5 G; and gain, 1×10^5.

(Figure 6C), further indicating that this radical has low solvent accessibility. By subtracting the spectrum obtained in the absence of DMPO (Figure 6C) from the spectrum obtained in its presence (Figure 6B), it was possible to observe a different EPR spectrum (Figure 6D). The spectrum obtained by subtraction varied somewhat with incubation time but always presented a value of a^{β}_{H} around 19 G. This value is consistent with DMPO-oxygen centered radical adducts other than the DMPO tyrosyl radical adduct and is somewhat higher than those expected for DMPO sulfur centered adducts (*33*). It is possible that the subtraction spectrum is a composite of more than one DMPO radical adduct due to the observed variability of the spectrum with incubation time. In this case, the most likely candidates are DMPO/•OTrp-BSA and DMPO/•SCys-BSA radical adducts. The latter, because BSA-CysS• radical production appears to precede the formation of the BSA-Tyr• radical produced in the presence of NO_2^- (Figure 4), whereas production of DMPO/•OTrp-BSA would be consistent with previous studies showing that BSA exposition to gaseous $^{\bullet}NO_2$ for several hours led to extensive damage of its tryptophan and tyrosine residues (*37*). Under our experimental conditions, however, tryptophan residues were not as extensively modified as ascertained by parallel experiments monitoring their fluorescence decay. After 30 min incubation, fluorescence losses were ca. 30% of the initial value (data not shown). This result may explain the low yields of the putative DMPO/•OTrp-BSA radical adduct produced in incubations of Cu,Zn-SOD/H_2O_2/NO_2^- (Figure 6B−D).

In conclusion, the spin trapping experiments confirmed the direct EPR studies by demonstrating that the main radicals produced from BSA treated with Cu,Zn-SOD/H_2O_2 in the presence of HCO_3^- or NO_2^- were solvent-exposed and -unexposed BSA-Tyr• radicals, respectively. Accordingly, $CO_3^{\bullet-}$ is a hydrophilic radical, whereas $^{\bullet}NO_2$ is a hydrophobic one (*20*). Taken together, these results indicate

Table 1: Rate Constant of Carbonate Radical Anion and Nitrogen Dioxide Reactions with Amino Acids and Peptides

radical	reactant	rate constant ($M^{-1}s^{-1}$) (pH)	ref
$CO_3^{\bullet-}$	Cys	4.6×10^7 (7.0)	*38*
	Tyr	4.5×10^7 (7.0)	*38*
	Trp	7.0×10^8 (7.0)	*38*
	His	5.6×10^6 (7.0)	*38*
$^{\bullet}NO_2$	Cys	5.0×10^7 (7.4)	*39*
	Gly-Tyr	3.2×10^5 (7.5)	*40*
	Gly-Trp	1.0×10^6 (6.5)	*40*

that the oxidants produced from Cu,Zn-SOD/H_2O_2/HCO_3^- and Cu,Zn-SOD/H_2O_2/NO_2^- are the diffusible $CO_3^{\bullet-}$ and $^{\bullet}NO_2$, respectively.

Oxidation of BSA by Two-Electron Mechanisms. The previous conclusion, however, does not completely explain the almost absent detection of the BSA-Cys• radical by spin trapping experiments with DMPO (Figure 6). Indeed, DMPO has been shown to be an efficient trap of protein-Cys• radicals (*24*, *30*, *31*). In addition, the blockage of BSA-cysSH completely inhibited detection of BSA-Tyr• in NO_2^- containing incubations (Figure 4), and cysteine reacts fast with both $^{\bullet}NO_2$ and $CO_3^{\bullet-}$ (Table 1) (*20*, *38*−*40*). Apparently, the oxidation level of BSA-CysSH in the incubations containing Cu,Zn-SOD/H_2O_2/HCO_3^- or Cu,Zn-SOD/H_2O_2/NO_2^- was not dependent only on the produced oxidants but also on the incubation components.

Indeed, BSA-CysSH is known to be oxidized by H_2O_2 by two-electron mechanisms albeit at relatively slow rates (k = 1.14 M^{-1} s^{-1}, pH = 7.4, 37 °C) (*41*). The high concentrations of H_2O_2 and BSA present in our reaction mixtures, however, led to a considerable BSA-cysSH oxidation in the time scale of most EPR experiments (1−15 min) even in the absence of the anions (Figure 7). Practically the same results were obtained in the presence and absence of Cu,Zn-SOD/H_2O_2 (data not shown) and in the presence and absence of NO_2^- (Figure 7), demonstrating that H_2O_2 itself is responsible for most of BSA-CysSH oxidation. Bicarbonate, however, was able to accelerate the rate of BSA-CysSH oxidation by H_2O_2 in the presence or absence of Cu,Zn-SOD (Figure 7). This suggests that HCO_4^- is probably being produced at the BSA-solvent interface (*17*, *18*).

BSA-CysSH oxidation by both H_2O_2 (*41*) and HCO_4^- (*17*, *18*) should proceed by two-electron mechanisms to produce the corresponding sulfenic acid (BSA-CysSOH) that has been recently shown to be remarkably stable in the case of human serum albumin (*42*). To prove BSA-CysSOH formation in our incubations, they were treated with NDB-Cl and analyzed UV−vis spectrophotometry as described in Experimental Procedures (Figure 7, inset). As expected, untreated BSA presented the absorption maximum at 400 nm characteristic of the thiol adduct (BSA-CysSNDB) (*42*, *43*). BSA incubated 7 min with either H_2O_2, Cu,Zn-SOD/H_2O_2, or Cu,Zn-SOD/H_2O_2/NO_2^- presented practically the same spectrum after NDB-Cl treatment. This spectrum is exemplified in the inset in Figure 7 as the spectrum obtained from Cu,Zn-SOD/H_2O_2/NO_2^-. The spectrum presented a decrease in the 400 nm peak and a new band at 358 nm that is characteristic of the sulfenic acid adduct (BSA-CysSONDB) (*42*, *43*). BSA incubated with Cu,Zn-SOD/H_2O_2/HCO_3^- presented similar spectral changes upon treatment with NDB-Cl, but the spectrum was broad,

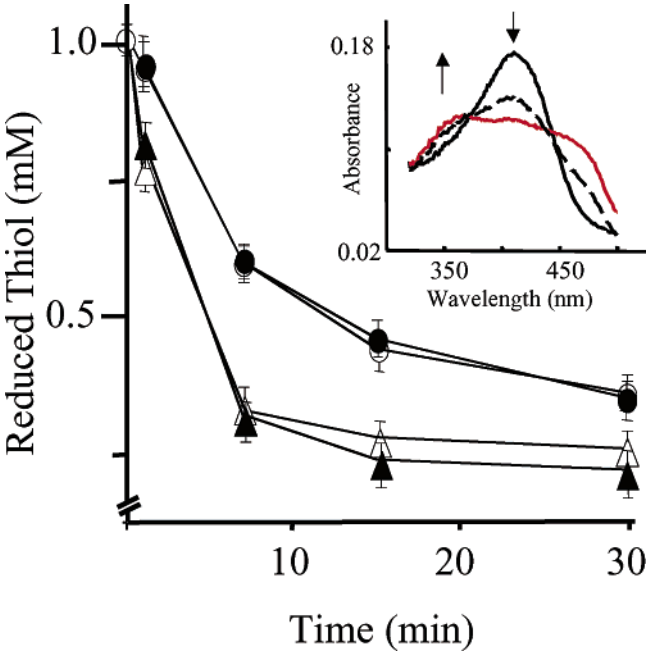

FIGURE 7: Kinetics of BSA thiol oxidation in different incubations. To BSA (100 mg/mL) in phosphate buffer (250 mM), pH 7.4, was added H_2O_2 (2.5 mM) plus Cu,Zn-SOD (2.5 mg/mL) (●); H_2O_2 (2.5 mM) plus Cu,Zn-SOD (2.5 mg/mL) plus NO_2^- (50 mM) (○); H_2O_2 (2.5 mM) plus HCO_3^- (50 mM) (△); and H_2O_2 (2.5 mM) plus Cu,Zn-SOD (2.5 mg/mL) plus HCO_3^- (50 mM) (▲). The inset shows the UV−vis spectra of the NDB adducts of native BSA (—) and BSA after 7 min incubation with Cu,Zn-SOD (2.5 mg/mL), H_2O_2 (2.5 mM), and NO_2^- (50 mM) (- - -) or with Cu,Zn-SOD (2.5 mg/mL), H_2O_2 (2.5 mM), and HCO_3^- (50 mM) (red line). Measurement of thiol oxidation and reaction with NDB−Cl were performed as described in Experimental Procedures. The shown values are mean ± standard deviations of the values obtained in three independent experiments.

and a band at 475 nm became more pronounced (Figure 7, inset). Presumably, this band is due to adducts of NDB with protein-amino groups although they are usually produced under alkaline conditions (*44*). Most likely, BSA denaturation is facilitating the NDB-Cl reaction with amino and other protein groups, particularly in the presence of HCO_3^-. A tyrosine adduct of NDB-Cl whose production is also facilitated at alkaline conditions has been described, but it presents a peak at 385 nm (*45*). In addition to cysteine, methionine is another BSA residue that is oxidized by H_2O_2 (*46*). The corresponding product, methionine sulfoxide, however, did not produce a NDB-Cl adduct under the present experimental conditions (data not shown).

Overall, the results summarized in Figure 7 show that under our experimental conditions, most of BSA-CysSH is oxidized by H_2O_2 to produce the corresponding BSA-CysSOH. In the incubations containing Cu,Zn-SOD/H_2O_2/NO_2^-, production of the BSA-CysS$^{\bullet}$ radical followed by fast electron transfer from a tyrosine residue (Figure 4) should occur in parallel with BSA-CysOH because c.a. 50% of BSA-CysSH is available as the thiol up to 15 min incubation (Figure 7). In contrast, the nondetection of BSA-CysS$^{\bullet}$ in incubations containing HCO_3^- in the presence of DMPO (Figure 6) was probably due to the faster oxidation to the BSA-CysOH (Figure 7). This group, being already oxidized, will render products that are oxidized beyond the sulfenic acid level.

DISCUSSION

Our results showed that BSA is oxidized to protein radicals during the peroxidase activity of Cu,Zn-SOD in the presence of HCO_3^- or NO_2^- (Figures 1−6). Since the production of BSA radicals requires oxidants that are diffusible and radicals themselves, the results demonstrate that the oxidants produced by Cu,Zn-SOD/H_2O_2/HCO_3^- and Cu,Zn-SOD/H_2O_2/NO_2^- are $CO_3^{\bullet-}$ and $^{\bullet}NO_2$ radicals, respectively. Accordingly, the main BSA radicals detected in each system were those expected from the known physicochemical properties of the generated diffusible radical (eqs 1−6) (Table 1) (see ref *20* for a review) and from the BSA structure (20 tyrosine, two tryptophan, and one thiol free cysteine) (*47*). Cu,Zn-SOD/H_2O_2/HCO_3^- produced a solvent-exposed BSA-Tyr$^{\bullet}$ radical (Figure 1) as inferred form its low instantaneous concentration throughout incubation (Figure 2) and its efficient trapping by both DBNBS (Figure 5) and DMPO (Figure 6). Production of a solvent-exposed BSA-Tyr$^{\bullet}$ radical is consistent with BSA attack by the hydrophilic $CO_3^{\bullet-}$ (*20*). In contrast, Cu,Zn-SOD/H_2O_2/NO_2^- produced a solvent-unexposed BSA-Tyr$^{\bullet}$ radical (Figure 3) as indicated by its accumulation during incubation time (Figure 2), its inefficient trapping by DBNBS (Figure 5), and its nontrapping by DMPO (Figure 6). In this system, low yields of a BSA-Trp$^{\bullet}$ radical also appeared to be produced (Figure 6D). Production of a solvent-unexposed BSA-Tyr$^{\bullet}$ and BSA-Trp$^{\bullet}$ radical is consistent with BSA attack by the hydrophobic $^{\bullet}NO_2$ (*20*).

The considerable protection afforded by NO_2^- as compared with that by HCO_3^- on Cu,Zn-SOD activity (Figure 2, inset) can also be explained by the radicals produced during the peroxidase activity of the enzyme. In the absence of anions, the active site histidine is oxidized by the metal-bound one-electron oxidant (Cu(II)$^{\bullet}$OH, Cu(I)O, or Cu(III)) (eq 4). In the presence of HCO_3^-, enzyme-bound histidine oxidation by $CO_3^{\bullet-}$ ($E = 1.78$ V, pH 7.0) (*20*), a strong one-electron oxidant, is likely to be as efficient as in its absence (*14*). Conversely, in the presence of NO_2^-, the enzyme-bound histidine is protected because $^{\bullet}NO_2$ ($E = 0.99$ V, pH 7.0) (*20*, *48*) is only a moderate one-electron oxidant.

Collectively, our results (Figures 1−6) add to the previous evidences supporting that the oxidant produced from Cu,Zn-SOD/H_2O_2/HCO_3^- is the diffusible $CO_3^{\bullet-}$ (*11*−*15*) and not an enzyme-associated HCO_4^- that may be converted to an enzyme-bound $CO_3^{\bullet-}$ as recently proposed (*16*).

In this context, the nondetection of the BSA-CysS$^{\bullet}$ radical by spin trapping experiments with DMPO (Figure 6) was at first surprising. In NO_2^- containing incubations that produced the solvent-unexposed BSA-Tyr$^{\bullet}$ radical only when BSA-CysSH was available for oxidation (Figure 4A,C), probably DMPO was not able to compete with the fast electron transfer from a solvent-unexposed tyrosine residue to BSA-CysS$^{\bullet}$ to produce the detected BSA-Tyr$^{\bullet}$ radical. However, BSA-CysS$^{\bullet}$ was also expected to be produced in HCO_3^- containing incubations because the generated $CO_3^{\bullet-}$ reacts fast with cysteine (Table 1). In addition, BSA-CysSH should be accessible to $CO_3^{\bullet-}$ because it is oxidized by the negatively charged peroxynitrite (*24*, *26*, *41*, *42*). This contradiction was resolved with the demonstration that under the experimental conditions employed, BSA-CysSH was oxidized by H_2O_2 to the corresponding sulfenic acid (BSA-CysSOH) in a

process that was accelerated by HCO_3^- (Figure 7). Thus, in the Cu,Zn-SOD/H_2O_2/HCO_3^- system, a considerable fraction of BSA-CysSH is present as BSA-CysSOH even at early incubation times. Oxidation of BSA-CysSOH beyond the sulfenic acid level is probably favored over BSA-CysSH oxidation to the BSA-CysS$^\bullet$ radical, justifying its nonproduction/detection by spin trapping experiments with DMPO (Figure 6A).

The demonstration that HCO_3^- accelerates BSA-CysSH oxidation by H_2O_2 to produce BSA-CysSOH in the absence of Cu,Zn-SOD (Figure 7) (see also Results) constitutes further proof that HCO_4^- is a two-electron oxidant (*17*, *18*). Also, it provides experimental support to the view that HCO_4^- may be an important biological oxidant whose production from H_2O_2 and HCO_3^- would be facilitated at protein− and membrane−water interfaces (Figure 7) (*17*, *18*). This is an important finding given the ubiquity and high physiological concentration of HCO_3^- and the pivotal role of protein thiol oxidation in the activation and deactivation of cell signaling pathways (*49*−*51*). Certainly, further studies about the production and biological roles of HCO_4^- are warranted.

Finally, it is relevant to emphasize that the systems, Cu,Zn-SOD/H_2O_2/HCO_3^- and Cu,Zn-SOD/H_2O_2/NO_2^-, provide an enzymatic pathway for the independent production of $CO_3^{\bullet-}$ and $^\bullet NO_2$, respectively. These radicals are being increasingly recognized to play a role in pathophysiological protein oxidation and nitration, but the mechanisms by which they promote these protein alterations remain obscure (*20*, *52*). This is due in part to the fact that their known biological sources produce them in parallel with other one-electron oxidants. For instance, peroxynitrite/CO_2 produces a flux of both $CO_3^{\bullet-}$ and $^\bullet NO_2$, whereas hemeperoxidases/H_2O_2/NO_2^- produce $^\bullet NO_2$ in parallel with hemeperoxidase compounds I and II that are also strong one-electron oxidants (*20*). Thus, the systems studied here can be useful to explore the mechanistic aspects of protein oxidation and protein nitration.

ACKNOWLEDGMENT

We thank Dr. Alícia J. Kowaltowski for helpful comments.

REFERENCES

1. Fridovich, I. (1989) *J. Biol. Chem. 264*, 7761−7764.
2. Hodgson, E. K., and Fridovich, I. (1975) *Biochemistry 14*, 5299−5303.
3. Hodgson, E. K., and Fridovich, I. (1975) *Biochemistry 14*, 5294−5299.
4. Yim, M. B., Chock, P. B., and Stadtman, E. R. (1993) *J. Biol. Chem. 268*, 4099−4105.
5. Uchida, K., and Kawakish, S. (1994) *J. Biol. Chem. 269*, 2405−2410.
6. Gunther, M., R., Peters, J. A., and Sivaneri, M. K. (2002) *J. Biol. Chem. 277*, 9160−9166.
7. Widedau-Pazos, M., Goto, J. J., Rabizadeh, S., Gralla, E. B., Roe, J. A., Lee, M. K, Valentine, J. S., and Bredesen, D. E. (1996) *Science 271*, 515−518.
8. Yim, M. B., Kang, J. H., Yim, H. S., Kwak, H. S., Chock, P. B., and Stadtman, E. R. (1996) *Proc. Natl. Acad. Sci. U.S.A. 93*, 5709−5714.
9. Liochev, S. I., Chen, L. L., Hallewell, R. A., and Fridovich, I. (1998) *Arch. Biochem Biophys. 352*, 237−239.
10. Valentine, J. S., and Hart, P. J. (2003) *Proc. Natl. Acad. Sci. U.S.A. 100*, 3617−3622.
11. Singh, R. J., Goss, S. P., Joseph, J., and Kalyanaraman, B. (1998) *Proc. Natl. Acad. Sci. U.S.A. 95*, 12912−12917.
12. Goss, S. P., Singh, R. J., and Kalyanaraman, B. (1999) *J. Biol. Chem. 274*, 28233−28239.
13. Zhang, H., Joseph, J., Felix, C., and Kalyanaraman, B. (2000) *J. Biol. Chem. 275*, 14038−14045.
14. Liochev, S. I., and Fridovich, I. (2002) *J. Biol. Chem. 277*, 34674−34678.
15. Zhang, H, Andrekopoulos, C., Joseph, J., Chaandran, K., Karoui, H., Crow, J. P., and Kalyanaraman, K. (2003) *J. Biol. Chem. 278*, 24078−24089.
16. Elam, J. S., Malek, K., Rodriguez, J. A., Doucette, P. A., Taylor, A. B., Hayward, L. J., Cabelli, D. E., Valentine, J. S., and Hart, P. J. (2003) *J. Biol. Chem. 278*, 21032−21039.
17. Richardson, D. E., Yao, H., Frank, K. M., and Bennet, D. A. (2000) *J. Am. Chem. Soc. 122*, 1729−1739.
18. Yao, H., and Richardson, D. E. (2003) *J. Am. Chem. Soc. 125*, 6211−6221.
19. Vásquez-Vivar, J., Denicola, A., Radi, R., and Augusto, O. (1997) *Chem. Res. Toxicol. 10*, 786−794.
20. Augusto, O., Bonini, M. G., Amanso, A. M., Linares, E., Santos, C. X. C., and De Menezes, S. L. (2002) *Free Radical Biol. Med. 32*, 841−859.
21. Andrus, P. K., Fleck, T. J., Gurney, M. E., and Hall, E. D. (1998). *J. Neurochem. 71*, 2041−2048.
22. Ferrante, R. J., Shinobu, L. A., Schulz, J. B., Matthews, R. T., Thomas, C. E., Kowall, N. W., Gurney, M. E., and Beal, M. F. (1997) *Ann. Neurol. 42*, 326−334.
23. Kaur, H., Leung, K. H. W., and Perkins, M. J. (1981) *J. Chem. Soc., Chem. Commun.*, 142−143.
24. Gatti, R. M., Radi, R., and Augusto, O. (1994) *FEBS Lett. 348*, 287−290.
25. Claiborn, A. (1985) in *Handbook of Methods for Oxygen Radical Research* (Greenwald, R. A., Ed.) pp 283−284, CRC Press, Inc., Boca Raton, FL.
26. Bonini, M. G., and Augusto, O. (2001) *J. Biol. Chem. 276*, 9749−9754.
27. Stubbe, J., and Van der Donk, W. A. (1998) *Chem. Rev. 98*, 705−762.
28. Ostdal, H., Andersen, H. J., and Davies, M. J. (1999) *Arch. Biochem. Biophys. 362*, 105−112.
29. Gunther, M. R., Sturgeon, B. E., and Mason, R. P. (2000) *Free Radical Biol. Med. 28*, 709−719.
30. Davies, M. J., Gilbert, B. C., and Haywood, R. M. (1993) *Free Radical Res. Commun. 18*, 353−367.
31. Clément, J.-L., Gilbert, B. C., Rockenbauer, A., and Tordo, P. (2001) *J. Chem. Soc., Perkin Trans. 2* 1463−1470.
32. Minetti, M., Scorza, G., and Pietraforte, D. (1999) *Biochemistry 38*, 2078−2087.
33. Li, A. S. W., Cummings, K. B., Roethling, H. P., Buettner, G. R., and Chignell, C. F. (1988) *J. Magn. Res. 79*, 140−142.
34. De Menezes, S. L., and Augusto, O. (2001) *J. Biol. Chem. 276*, 39879−39884.
35. Augusto, O., De Menezes, S. L., Linares, E., Romero, N., Radi, R., and Denicola, A. (2002) *Biochemistry 41*, 14323−14328.
36. Gunther, M. R., Tschirret-Guth, R. A., Witkowska, H. E., Fann, Y. C., Barr, D. P., Ortiz de Montellano, P. R., and Mason, M. P. (1998) *Biochem. J. 330*, 1293−1299.
37. Kikugawa, K., Kato, T., and Okamoto, Y. (1994) *Free Radical Biol. Med. 16*, 373−382.
38. Chen, S. N., and Hoffman, M. Z. (1973) *Radiat. Res. 56*, 40−47.
39. Ford, E., Hughes, M. N., and Wardman, P. (2002) *Free Radical Biol. Med. 32*, 1314−1323.
40. Prutz, W. A., Monig, H., Butler, J., and Land, E. J. (1985) *Arch. Biochem. Biophys. 243*, 125−134.
41. Radi, R., Beckman, J. S., Bush, K. M., and Freeman, B. A. (1991) *J. Biol. Chem. 266*, 4244−4250.
42. Carballal, S., Radi, R., Kirk, M. C., Barnes, S., Freeman, B. A., and Alvarez, B. (2003) *Biochemistry 42*, 9906−9914.
43. Ellis, H. R., and Poole, L. B. (1997) *Biochemistry 36*, 15013−15018.
44. Ghosh, P. B., and Whitehouse, M. W. (1968) *Biochem. J. 108*, 155−156.
45. Aboderin, A. A., and Boedefeld, E. (1976) *Biochim. Biophys. Acta 420*, 177−186.

46. Finch, J. W., Crouch, R. K., Knapp, D. R., and Schey, K. L. (1993) *Arch. Biochem. Biophys. 305*, 595−599.
47. Hirayama, K., Akashi, S., Furuya, M., and Fukuhara, K.-i. (1990) *Biochem. Biophys. Res. Commun. 173*, 639−646.
48. Koppenol, W. H., Moreno, J. J., Pryor, W. A., Ischiropoulos, H., and Beckman, J. S. (1992) *Chem. Res. Toxicol. 5*, 834−842.
49. Georgiou, G., and Masip, L. (2003) *Science 300*, 592−594.
50. Wood, Z. A., Poole, L. B., and Karplus, P. A. (2003) *Science 300*, 650−653.
51. Woo, H. A., Chae, H. Z., Hwang, S. C., Yang, K.-S., Kang, S. W., Kim, K., and Rhee, S. G. (2003) *Science 300*, 653−656.
52. Ischiropoulos, H. (2003) *Biochem. Biophys. Res. Commun. 305*, 776−783.

BI035606P